NFAL Prototype Design and Feasibility Analysis for Self-Levitated Conveyor Belt

Xiaoni Chang, Bin Wei, M. Atherton, Keyan Ning, C. Mares & T. Stolarski

NFAL Prototype Design and Feasibility Analysis for Self-Levitated Conveyor Belt

Xiaoni Chang[1], Bin Wei[2*] , M. Atherton[3], Keyan Ning[4]. C. Mares[3], T. Stolarski[3]

1School of Economic and Management, Beihang University, Beijing, China,100191

2 State Key Laboratory of Tribology, Tsinghua University, Beijing, China 100084

3.College of Engineering, Design and Physical Sciences, Brunel University, UK

4. National Key Laboratory of Vehicle Transmission, China North Vehicle Research Institute, Beijing 100072, China

Abstract：In order to avoid friction and scratch of the cans on the conveyor belt, an acoustic levitation prototype was designed, so as to verify the feasibility in the can transportation. The modal shapes and the forced harmonic shapes of the prototype are obtained by the ANSYS coupled field computation with ¼ symmetry model and the levitation capacity was carried out by the use of groups of stimulation and test instruments. The simulation results showed that the pure flexural and mixed flexural wave shapes with different wave number existed at some specific frequency. The amplitude in the central point can only be stimulated when resonant in few frequencies by the four piezo-electric disks that are glued at the bottom of the aluminium plate, which can be observed in the frequency spectrum. The experimental results confirmed the theoretical results and the feasibility of the prototype, the same time, confirmed that objects can be floated in several resonant frequencies under forced vibrating condition. The situation that the system can provide largest bearing capacity is when both the piezo-electric disc and the plate could vibrate resonantly at the same time.

Keywords: NFAL; ANSYS; Prototype; Resonant; Piezoelectric

---

* Corresponding author. buaaweibin@126.com

1 Introduction

The NFAL (Near Field Acoustic Levitation) concept is come from the high frequency gas squeeze theory. The gas squeeze theory is originally proposed by Gross[1] and improved by Langlois[2]. Next, E.O.J.Salbu[3] proposed the fixed object squeeze film model and believed that the squeeze film characteristics is similar with the piston exciting situation. The carrying capacity can be obtained by simple calculation. The free levitation theory is first proposed by Beck JV[4] and numerical method is applied in his model. Later, the research about squeeze film characteristics which was solved by lubrication dynamic methods was developed for years[5,6].Based on free levitation theory, the modal shapes was considered in Yoshiki.Hashimoto's research[7]. The excited shape was supposed ideal flexural wave and the film thickness equation was coupled by it. The model was proved to be more stable and higher bearing capacity than that in the rigid disk excitation condition. Later, the linearization solution was derived by Minikes and Bucher[8] and the feasibility was verified by Yoshiki.Hashimoto's experiments results. Stolaski and Wei Chai investigated the characteristics of the designed linear bearing, and then, the 2D model for the new bearing was established gradually [9,10].LI jin, LIU Pinkuan etc[11,12]researched the bearing force in experiments and achieved the film thickness curves versus frequencies. Recently, some scholars combined the squeeze film theory with ultrasonic phenomenon [13]-[16] and compared the ultrasonic levitation results with squeeze film by numerical computation. Thus, the concept 'ultrasonic squeeze film' was proposed and the theory was further developed. Recently, from the point of view of engineering practice, lots of researchers focus on some typical situations of the squeeze film such as the Non Newtonian fluid

film, the film with porous layer, damping effect and so on[17]-[19].The whole research histories for the near field acoustic Levitation are listed in Tab.1.

The listed table showed different model and solution method for the NFAL system. Aiming at the model forms, there are three main models for the NFAL system; they are infinite width model for simply estimating, axial Symmetry model for the round exciting disc and 2-D model for common exciting plate. All of the modal shapes, including rigid, pure flexible, mixed (true) models and object status could influence the complex extent of the mathematic models. The solutions corresponding to the models mainly included acoustic radial field and squeeze film methods, however, for the free object only can the model solved by the numerical way.

In the engineering practice, the horn is helpful to the actuator design [20]. But due to the space constraints, the designable horn cannot be used in the conveyor self-levitation system, so the resonance frequency of the system is difficult to predict and affected a lot by the layout of the piezo-discs.

2 Prototype Design

The real physical NFAL platform and the levitated samples are shown in Fig.1. The dimension and the materials of the piezo-electric discs and the exciting plate are listed in Tab.2. The four piezo-electric discs are connected with the output port of the amplifier by the block terminal with a 1 Ampere fuse. The layout of piezo-electric discs is shown in Fig.2.

The piezo-electric discs are fixed at the bottom of the plate with professional glue, and then a distress treatment lasted for 12 hours. So, the prototype of the actuator (exciting plate) is made up of the plate and the piezo-electric discs which can eradiate sonic field and squeeze the gas

ACCEPTED MANUSCRIPT

which is close to the plate surface. In this circuit, the capacitances are parallel connected, whose resonant frequency is determined by the total capacitances and equivalent inductances. The system characteristics are concerned more than the single piezoelectric disc. The system resonance frequency and impedance are more important to the levitation capacity than the properties of the piezoelectric discs. Many kinds of levitation samples including metallic and non-metallic are chosen to test the levitation effects in the experiment. The designed plate actuator is shown in Fig.3. The floating objects on the plate can be self-levitated by the effect of NFAL.

3. The plate finite element and the squeeze film model of the piezoelectric plate actuator

Due to the air pressure boundary condition is neglected in the FEM model of the exciting pate, it is reasonable to calculate the modal and harmonica shapes first, and then obtain the accurate film thickness equations coupled with the plate shapes, by which, calculate the bearing force (nodes pressure) by the Reynolds equation coupled with the film thickness equation.

3.1 The Finite element model of the exciting plate

The deforming shapes of the plate actuator can be carried out by the finite elements model. The mathematical model is determined by the geometric dimensions of the plate and the piezoelectric discs (Fig.2). The FEM vibration model for PZT-4 was researched theoretically and experimentally. It was proved to be accurate of the ANSYS FEM model by comparing the results of disc excitation experiments [20]. The finite element model and boundary condition of the exciting plate are shown in Tab.3. The materials parameters are listed in Tab.4. The model coupled with electric-structure would be better simulating the real experiment status. Three

materials are included, that is aluminium, brass linings and PZT4 which are glued with each other in the ANSYS Pre-treatment. In the Engineering practice, the symmetry modal shapes (either with XZ or YZ plane) are available to ensure the cans are able to steadily self-levitation in the central area on the conveyor belt. So, only a quarter of the geometer is meshed due to the symmetry structure, by which, some of the irregular modes would be missed, but it is benefit to the main modes extracted from the multiplex ones. The model is divided into different partitions to ensure the hexahedral mesh by the sweeping method. There boundary conditions are applied in this model, they are fixed boundaries on the left side of the plate, symmetry boundaries on the XZ and YZ Plane and 5 Volt difference on the each side of the piezo-electric disc. The static, modes and harmonic results of the disk can be obtained by the ANSYS electric-structure-coupling analysis.

The key Input parameters for the metal and PZT materials are listed as Tab.4

3.2 The squeeze film model of the actuator

The infinite width squeeze film governing equations for fixed floating object consisted of Reynolds equation and film thickness ones. The film thickness equation should be defined by the shapes of the plate at a special frequency. Due to the dimension of the exciting plate and the actual form of the conveyor belt, it is reasonable to calculate with infinite wide mode.

The film thickness equations with pure flexural modes are shown as Fig.4.

Where, N is wave number, which means the number of wavelength in the exciting plate. Y is the modal shapes equation in order to determine the position of the vibration point.

So, the dimensionless governing equations for the infinite width plate are listed as follows:

The dimensionless film thickness equation:

$$H(X,T) = 1 - Y(X) \cdot \sin T \dots\dots\dots\dots\dots\dots\dots\dots\dots\dots\dots..1$$

And the Reynolds equation:

$$\frac{\partial}{\partial X}\left(PH^3 \frac{\partial P}{\partial X}\right) = \sigma \frac{\partial(PH)}{\partial T} \dots\dots\dots\dots\dots\dots\dots\dots\dots\dots\dots\dots\dots\dots\dots2$$

Where, the dimensionless parameters $H = \dfrac{h}{h_0}$, $X = \dfrac{x}{L} \in (0, 1)$, $P = \dfrac{p}{p_a}$, $T = \omega t$, $\sigma = \dfrac{12\mu\omega b^2}{h_0^2 p_a}$

(squeeze number), $Y(X) = a \cdot \sin(2\pi N \cdot X)/h_0$

For the square sample, the bearing force can be derived by the pressure integral, as follows

$$f_1(T) = \iint\limits_{S_1} (p - p_a)dxdy = \int_0^a \int_0^b (p - p_a)dxdy \dots\dots\dots\dots\dots\dots\dots\dots3$$

Where, S_1 is the square integral area; a, b are the length and the width respectively.

For the round sample, the pressure integral can be derived as

$$f_2(T) = \iint\limits_{S_2} (p - p_a)rdrd\theta = \int_0^{R_0} \int_0^{2\pi} (p - p_a)rdrd\theta \dots\dots\dots\dots\dots\dots\dots..\dots\dots\dots4$$

Where, S_2 is the round integral area; R_0 is the radial of the sample; $x = r\cos\theta$, $y = r\sin\theta$.

The program flow chart is shown as Fig.5. The Reynolds equation was calculated by the means of centre difference and coupled with the film thickness equation including the plate deformation.

4 Results and discussion

The modal shapes calculated by ANSYS are listed in Tab.5 (below 15 kHz). The Symmetry model can explain the basic forms for the exciting plate. There are three kinds of modal shapes.

First, they are the pure flexural mode along *X* direction such as Mode 1st, 3rd, 5th and so on. Second, they are the pure flexural modes along *Y* direction such as 2nd, 6th, 12th, and so on. The last are mixed wave shapes with different wave number along *X* and *Y* direction. For example, the fourth step of modal shapes show the 1.5*1 mixed wave shapes.

For the convey belt, the larger amplitude in the central line of the plate are needed. The forced harmonica spectrum on origin point (central point) is shown as Fig. 6. Not all of the modes can be stimulated well in the forced vibrating condition and also, not all of the peaks of vibrating amplitude are the natural modes, but some are the harmonica modes. The amplitude-frequency curves showed the magnitude trend with the increase of the frequency. Nearly all the modal shapes can be excited, but with different magnitude. The harmonica results are corresponding with the modal shapes. But the resonant frequency is different a little due to the coupling effect of piezo-electric materials.

5 Experiments and verification

The experiments instruments are shown in Fig.7, including signal generator, power supply amplifier, oscilloscope, accumulator and millimetre. Some key parameters in the experiments are listed in Tab.6.

The harmonica shapes of the plate are test by the laser scanning vibrometer from Polytec Company. 41x25 total 1025 nodes are distributed on the plate to collect the velocity on Z (height) direction as Fig.8. The sweeping voltage is 5V.

The average velocity RMS on all surface nodes curves versus frequency is shown as Fig.9.Due to the symmetry mode in ANSYS, some of the harmonic resonance of the plate could be missing.

But the mainly levitation point and modal shapes were shown in the spectrum. By contrast to the experiments harmonica spectrum, we found that there are more irregular peaks in the experiments results due to the symmetry model in the theoretical analysis. The same, we extract the harmonica shapes below 15KHz frequency from the experiments. There corresponding plate deformations are listed in Tab.7.

By contrast to the simulation results in Tab.5, from Tab.7, we found that the symmetry model can better embody the modal shape of the plates. All of the shapes of peaks are included in the Tab.5 (theoretical one) when the frequency is below 15 kHz. The theoretical errors showed that all the simulation results of one fourth model against the experiments results are below 15%. The largest errors occurred at the ones along *X* direction (step 3, 5, 9) due to the simplified boundary condition. In opposite, the ones along *Y* direction have best accuracy due to the free boundaries. The experiment results showed that not all of the modal shapes can make the object self-levitated. The pure ones are appropriate for lower frequency while the mixed ones are appropriate for higher frequency. This phenomenon can explain that some researchers gave the different optimization modal shapes for the self-levitation of different structures and this result gave a significant guidance to the prototype design.

The displace results of the central point are shown in Fig.10. It is different with the RMS curves but have a same trend with it. By contrast with the harmonica simulation results (Fig.6), the results implied that the amplitude in the central point embodied the whole vibrating status to a certain extent.

The levitation experiment needs the amplifier to enlarge the energy input. The performance parameters of Fuji amplifier are listed as Tab.8. It can provide the fixed 15 times magnifying for all the D.C and A.C signal. It also can adjust the work point for obtaining the largest band for the experiments. The levitation height of the object was tested by the laser scanning sensor (in Fig.11). The levitation object is made of nylon, the dimension is Φ25mm X 3mm and the weight is 6g. For the largest energy output, the work point should be defined in the amplifier. The 7 volt offset (before amplify) can guarantee the largest amplitude and clipping does not appear in which, the oscilloscope can pride significant help in the experiments setup.

The experiment results and fitting curves are shown as Fig.12. All the experiment points are corresponding to the modal results in Tab.7 (Black Square). The results implied that the levitation can be achieved in 6 points in the frequency band, and other points are failed to levitate. The failed experiment points showed that the pure flexible wave is appropriate to achieve levitation in low frequency. In opposite, the mixed shapes are appropriate in higher frequency. This principle can guide and optimize the design of NFAL platform which work in different frequency band.

The fitting curve expression is an exponential function with 95% confidence bounds:

$F(x)$=32.2*exp(8.416e-6*x) -44.86*exp(-7.764e-4*x)………………………….……4

This expression can give the estimate levitation height of the object, the trend of the levitation curve is reasonable and corresponding to the theoretical results [7],[20]

ACCEPTED MANUSCRIPT

6 Conclusion

1) The plate actuator with four piezo-electric discs has considerable bearing force that it can be used in the can conveyor Belt.

2) Almost all of harmonica shapes can be expressed in the simulation of the one fourth models. The symmetry shapes have larger bearing force and the levitated object is more stable.

3) The mode design is determined by the range of work band, for the lower band, pure flexural modes are appropriate. In opposite, the mixed modes are benefit in higher frequency range.

4) For acquiring more energy from the amplifier, the working point should be set up to guarantee the largest amplitude and clipping did not appear.

5) The levitation height is an exponential function of frequency. It is consistent to the theoretical results
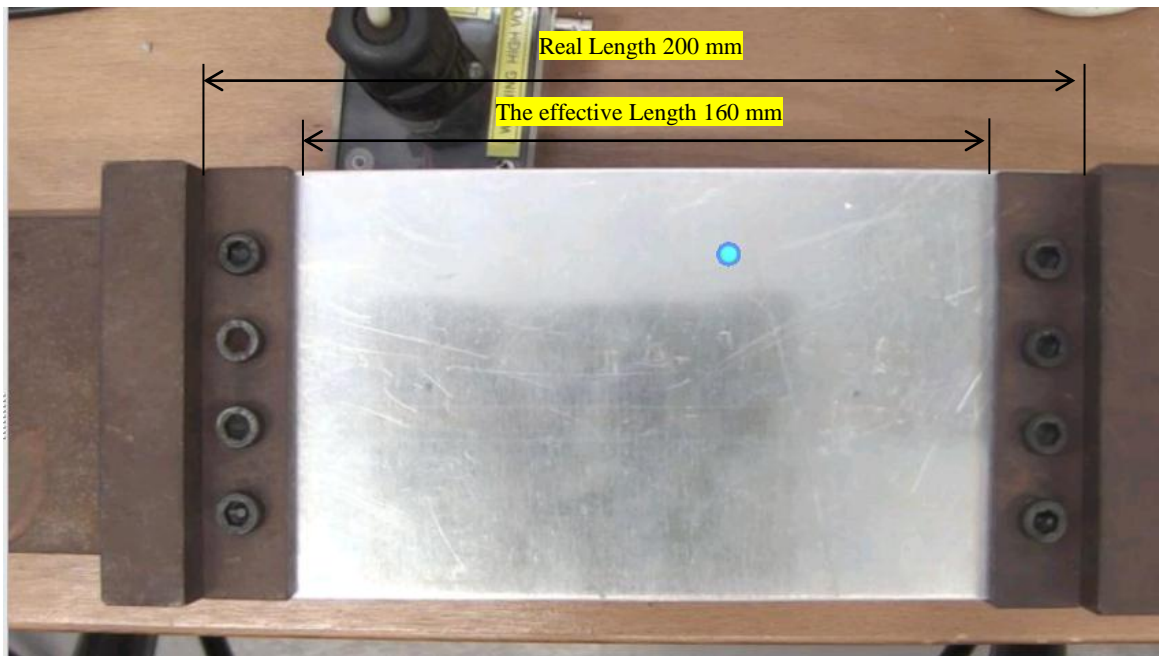
Fig.1 The designed plate actuator
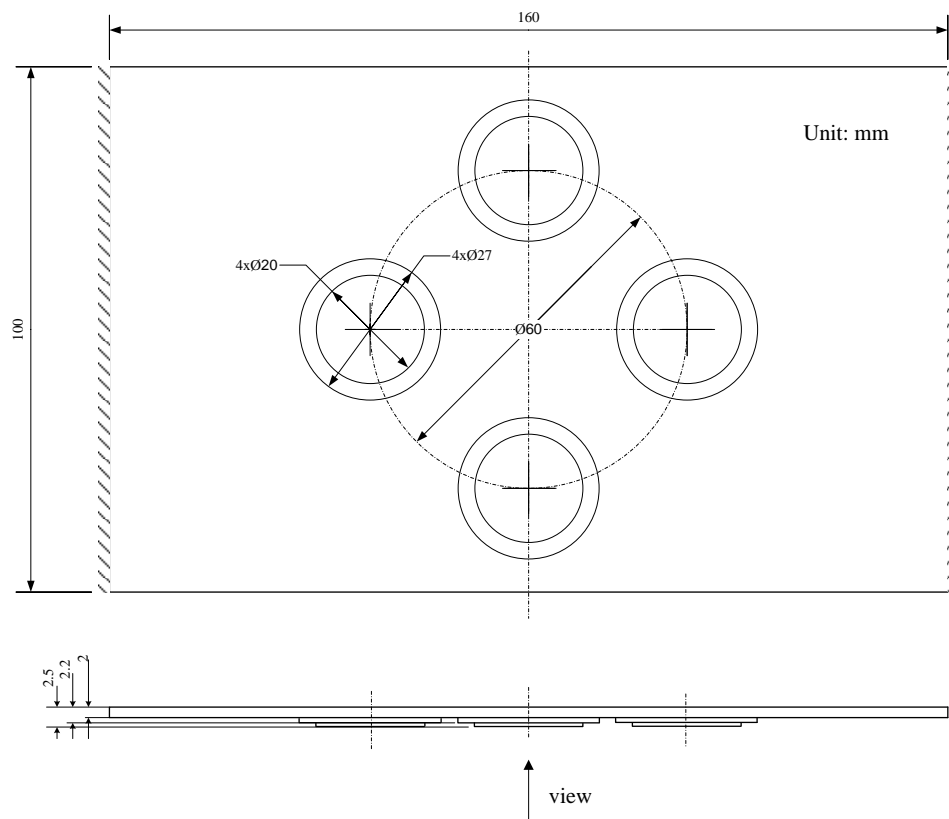
Fig.2 Dimension of the exciting plate

Fig.3 The levitation samples.

N=1.5 (Wave No.)

$y=asin[(2\pi*N/L)\cdot x]$

y

L

x
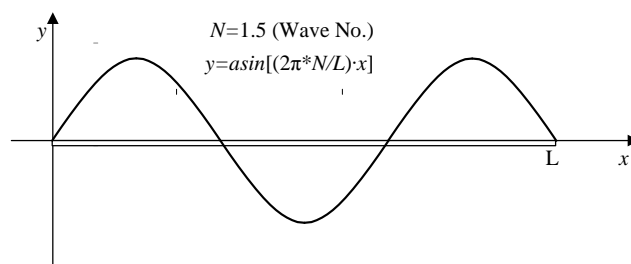
Fig.4 The theoretical model of the squeeze film
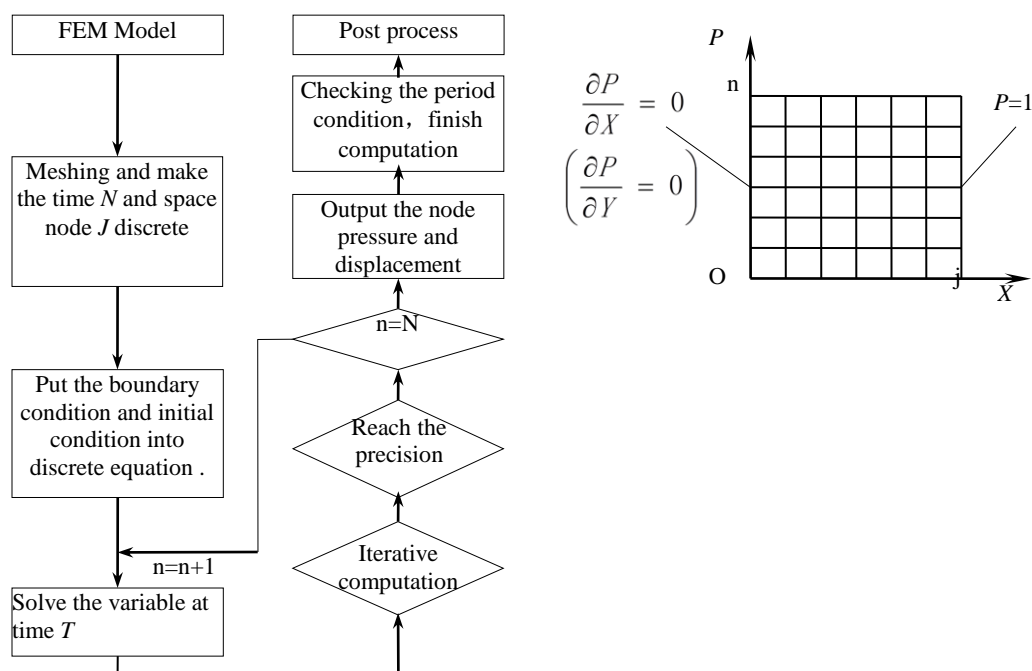
Fig.5 flowchart of the theoretical solving
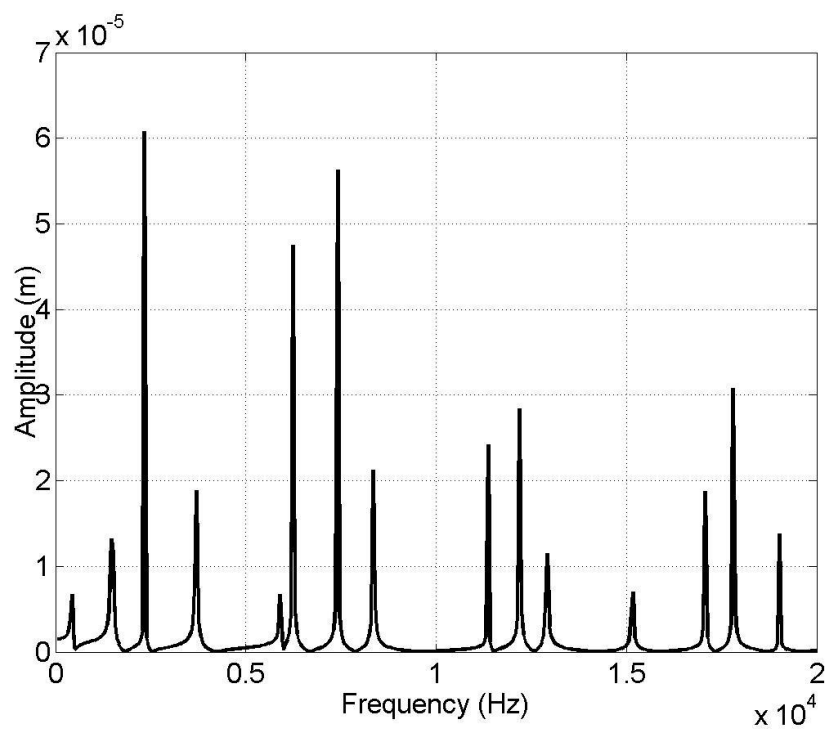
Fig.6 Harmonica analysis results of central point
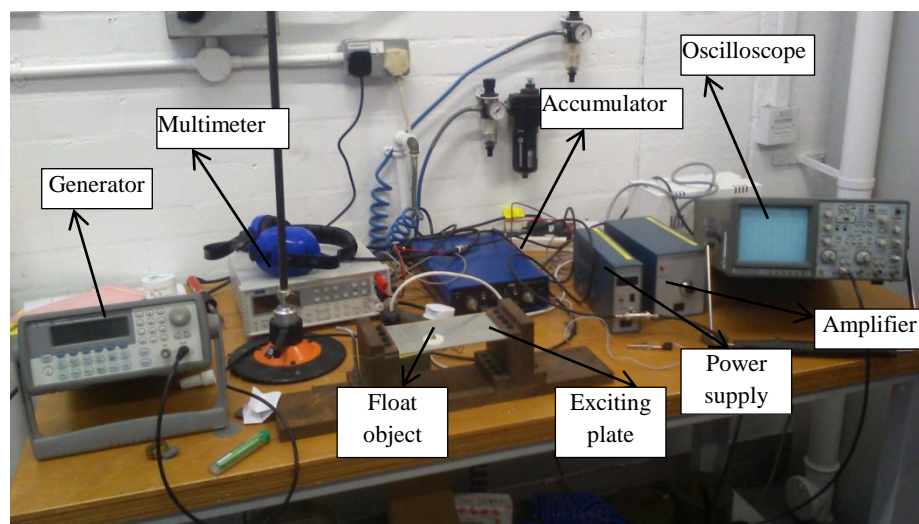
Fig.7 The layout of the experiments
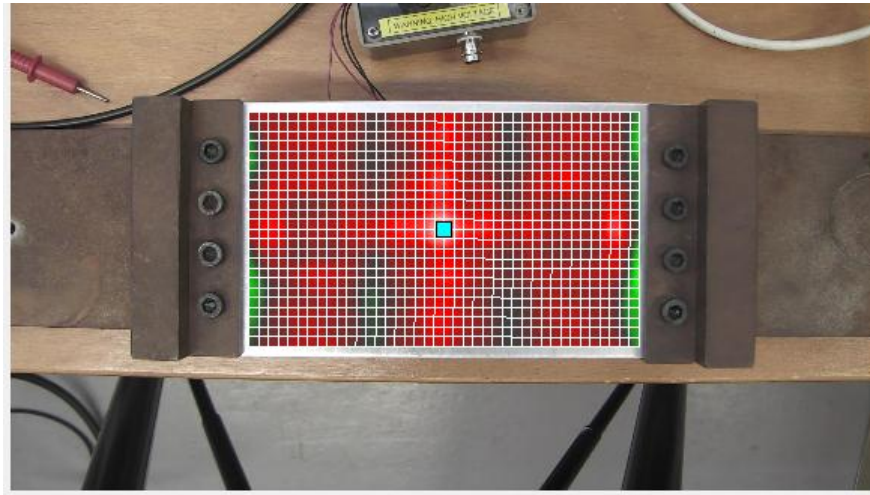
Fig.8 The mesh grid of the modal test
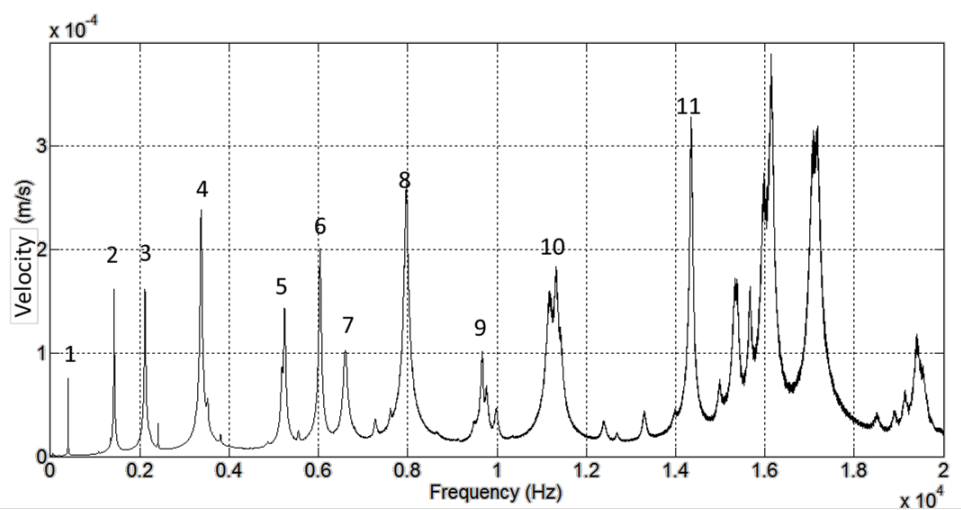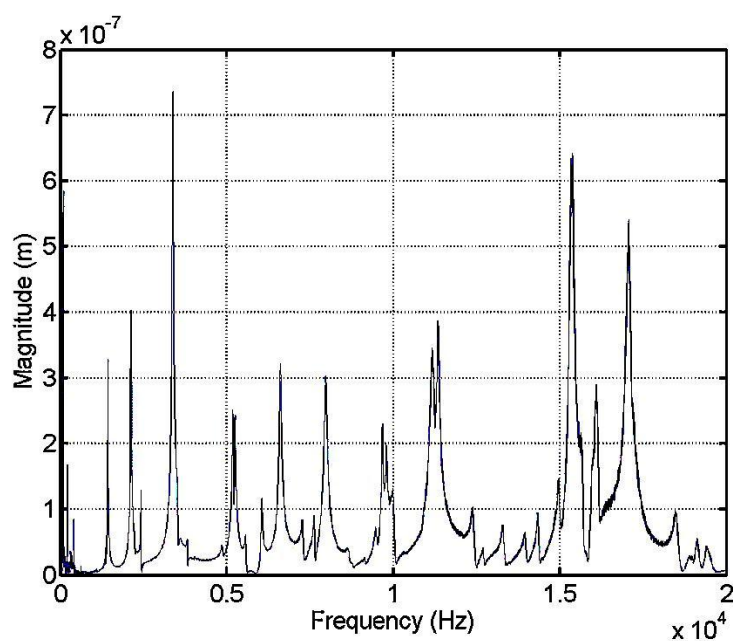
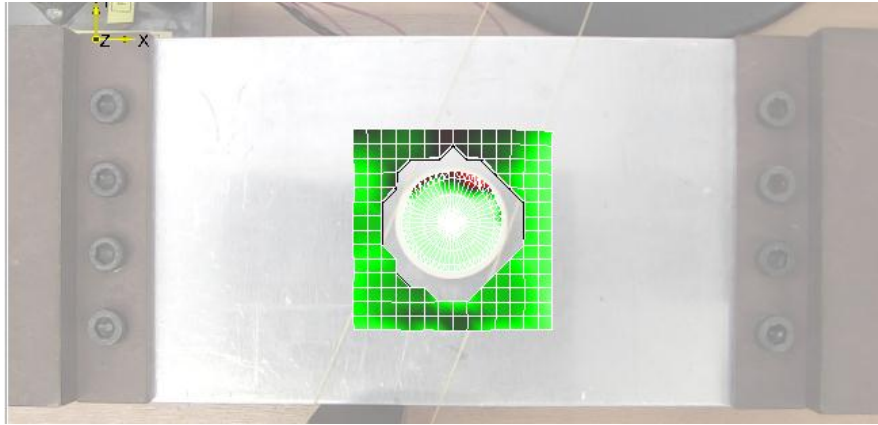Fig.9 The average velocity curves of experimental data

Fig.10 the experiment results of the central point

Fig.11 Mesh grid for the levitation height of the object measurement
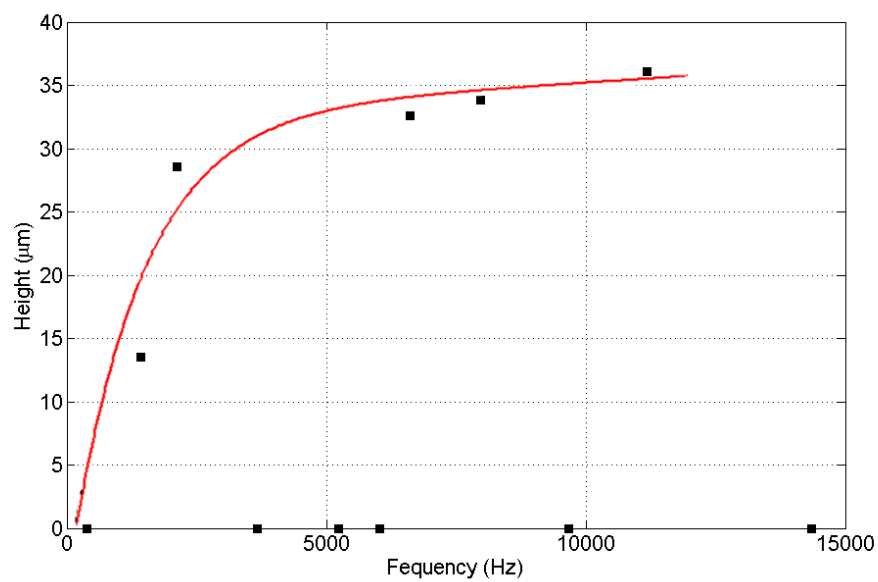
Fig.12 The levitation experiment results
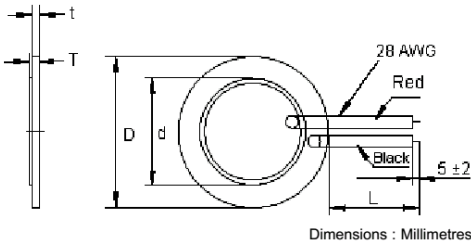
Tab.1 The research history of the NFAL

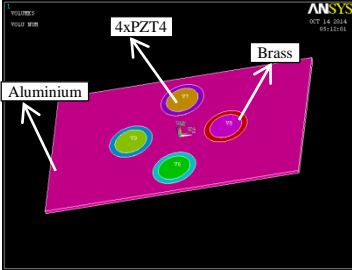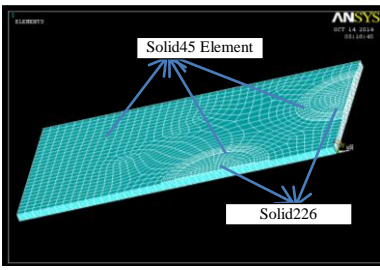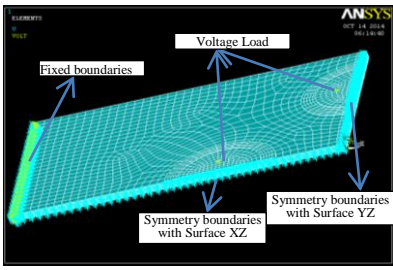| Publication Time	First Author	Model Type	Modal Shape of Excitation Disk	Sample suspended situation	Calculation method
1961	Langlois[2]	Infinite Wide Axial Symmetry	Not take account	Fixed	Reynolds equation perturbation
1964	Sablu[3]	Axial Symmetry	Not take account	Fixed	Reynolds equation numerical method
1968	Diprima[21]	Infinite Wide	Not take account	Fixed	Reynolds equation analytic method
1969	Beck[4]	Axial Symmetry	Not take account	Free	Reynolds equation and motion equation perturbation method
1983	Takada[22]	Infinite Wide	Not take account	Fixed	Reynolds equation linearization method
1984	Shigeaki.Kuroda[23]	Axial Symmetry	Not take account	Free	Numerical method

1996	Yoshiki .Hashimoto[7]	Infinite Wide	Flexible modal shape	Fixed	Ultrasonic analytical theory
1997	Beltman[24]	2D Rectangle	Not take account	Fixed	Finite element method
2003	Butcher[25]	Axial Symmetry	Flexible modal shape	Fixed	Numerical method
2004	Minikes[8]	Infinite Wide	Rigid and Flexible model	Fixed	Modified Reynolds linearization method
2006	Stolarski[9]	2D Model	Not take account	Fixed	Reynolds equation numerical method
2006	Stolarski[26]	2D Model	Flextrual model	Fixed	Experiment reserch
2007	Shigeka.Yoshimoto[27]	2D Model	Take account	Free	Reynolds equation numerical method ANSYS fluid simulation
2009	LIU Pinkuan[11]	Axial Symmetry	Flexible Wave	Fixed	Reynolds equation numerical method
2010	Stolarski[10]	2D Model	Take account	Free	Reynolds equation numerical method

Year	Author	Model	Modal shape	Boundary	Method
					ANSYS fluid simulation
2011	WEI Bin[28]	Axial Symmetry	Real modal shape	Fixed	ANSYS ultrasonic simulation
2012	Stolarski[29]	2D Model	take account	Fixed	Reynolds equation numerical method
2014	WEI Bin[20]	Axial Symmetry	Mixed modal shape	Free	Reynolds equation analytic and numerical method
2014	WEI Bin[30]	Infinite wide	Rigid model	Fixed	Reynolds equation linearization method

Tab.2 The dimension and the materials of the piezo-electric discs and the plate

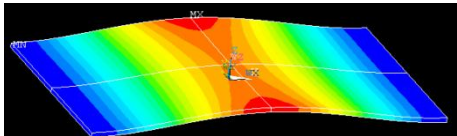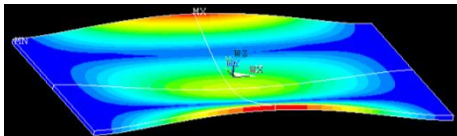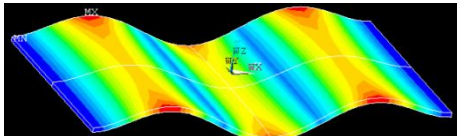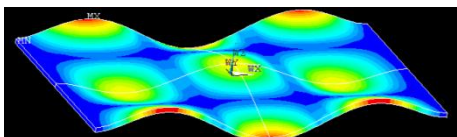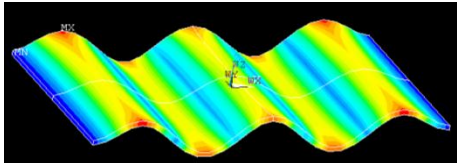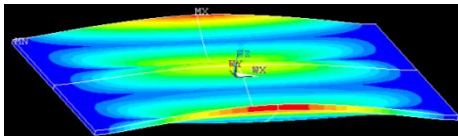| Sort	image	Drawing	Properties
Piezo-electric disc			Materials: Brass and iron Resonant frequency: 4.2K D:27mm d: 20mm t=0.3 T=0.5
Plate and layout		As Fig.2	Materials: Aluminium Real length:200mm Effective lenth:160mm Width:100mm Height:2mm

ACCEPTED MANUSCRIPT

Tab.3 The Finite model and boundary condition of the exciting plate

| Geometry and materials	Hexahedral mesh and element (1/4)	Boundary condition and Load (1/4)

Tab.4 The materials of the elements.

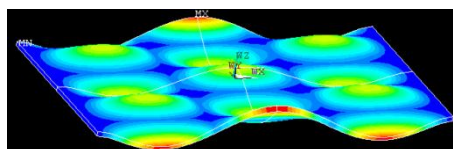| Materials	Dielectric constants	Young's Modulus (GPa)	Poisson 's ratio	Density (kg/m^3)	Piezoelectric voltage constants (C/m^2)
Aluminium	/	69	0.3	2700	/
Brass	/	110	0.3	6400	/
PZT4	$\begin{bmatrix} 804.6 & 0 \\ 0 & 804.6 \\ 0 & 0 \end{bmatrix}$	$\begin{bmatrix} 132 & 71 & 73 & 0 & 0 \\ & 132 & 73 & 0 & 0 \\ & & 115 & 0 & 0 \\ & & & 30 & 0 \\ & & & & 26 \end{bmatrix}$	/	7500	$\begin{bmatrix} 0 & 0 & -4.1 \\ 0 & 0 & -4.1 \\ 0 & 0 & 14.1 \\ 0 & 0 & 0 \\ 0 & 10.5 & 0 \\ 10.5 & 0 & 0 \end{bmatrix}$

Tab.5The modal shapes of the exciting plate

Model Frequency	Images Expand from 1/4	Explanation
1(417.9)		Pure flexural wave along *x* direction
2(1461.8)		Pure flexural wave along *y* direction
3(2291.3)		Pure flexural wave along *x* direction
4(3632.0)		Mixed modal with both *x* and *y* direction(1.5*1)
5(5794.0)		Pure flexural wave along *x*
6(6124.5)		Pure flexural wave along *y*
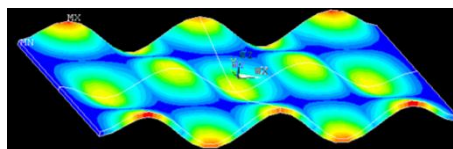
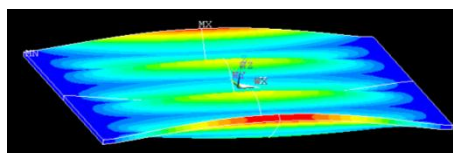|		
7(7274.8)		Mixed modal with both *x* and *y* direction(2.5*1)
8(8202.4)		Mixed modal with both *x* and *y* direction(2*1.5)
9(11128.9)		Pure flexural wave along *x*
10(11994.3)		Mixed modal with both *x* and *y* direction(2.5*2.5)
Not appeared in experiments (12662.9)		Mixed modal with both *x* and *y* direction(3.5*2)
11(14853.8)		Pure flexural wave along *y*
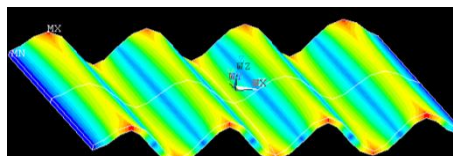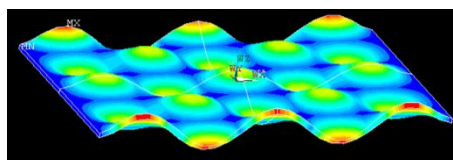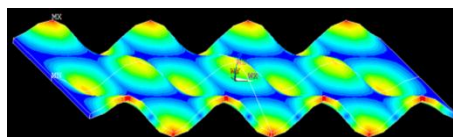
30
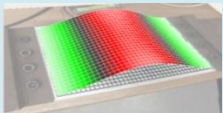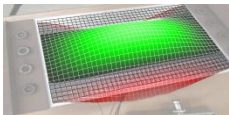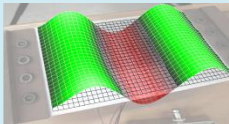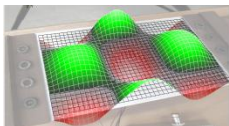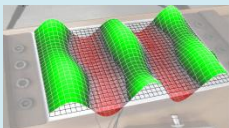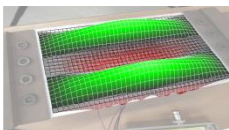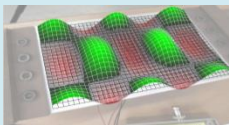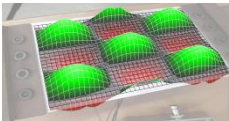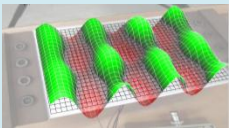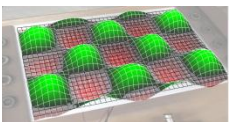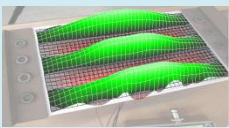
Tab.6 The Experiment parameters

Bandwidth:	Acquisition Mode:	Sample frequency:	Resolution:	Range:
50 kHz	FFT	128 kHz	1.953125 Hz	5 V

ACCEPTED MANUSCRIPT

Tab.7 the experiment results

Sequence	Frequency	Harmonica shapes	Magnitude (um)	Theoretical errors	Floating
1	393.7		75.12	5.8%	unavailable
2	1425.0		161.4	2.5%	available
3	2115.6		162.03	7.7%	available
4	3671.9		238.65	1.1%	unavailable
5	5240.6		143.04	9.5%	unavailable
6	6037.5		200.8	1.4%	unavailable
7	6612.5		102.35	9.1%	available

8	7965.6		264.42	2.9%	available
9	9668.8		101.19	13.1%	unavailable
10	11178.1		160.11	6.8%	available
11	14353.1		327.84	3.3%	unavailable

ACCEPTED MANUSCRIPT

Tab.8 The performance parameters of the Fuji amplifier and power supply.

Performance index	Range
Output Voltage	0-150V
Output Current	1A
Voltage range	0-+150V
Bandwidth	Dc-100KHz
	$(100V_{p-p}$ output)
Internal resistance	100KΩ
Amplification	25 dB(15 times)
The Stability to time	$1*10^{-4}$/h
The Stability to Current	$1*10^{-4}$
Dimension	103mm(W)*124mm(H)*220mm(D)
Weight	4.5Kg

ACCEPTED MANUSCRIPT

Reference

[1]Gross.W.A (1962). .Gas Film Lubrication, New York :Wiley.

[2]W.E.Langlois (1962). Isothermal Squeeze Films, Quarterly of Applied Mathematics. 1962.XX(2), pp 131-150

[3]Salbu EOJ (1964). Compressible squeeze films and squeeze bearings ASME J of Basic Eng, 86(3), pp 355-366

[4]Beck JV (1969). Experimental and analysis of a flat disk squeeze-film bearing including effects of supported mass motion,Holiday WG. ,Strodtman CL. ASME J of Lubr,91(1), pp 138-148

[5]Shigeaki.Kuroda,Noriyuki.Hirata (1984). Near field acoustic levitation of planar specimens using flexural vibration. J of Lubr. 50 (459), pp 2727-2731.

[6]M.Q JING, H LIU, Y SHEN, L YU (2008).Journal of Xi'an Jiaotong University, New Style Squeeze Film Air Bearing. 42(07), pp 799-802

[7]Yoshiki Hashimoto (1996). Near field acoustic levitation of planar specimens using flexural vibration. J.Acoust.Soc. 100(4), pp 2057-2061

[8]Adi Minikes,I Bucher (2004). Levitation force induced by pressure radiation in gas squeeze films. J.Acoust.Soc, 116(1), pp 217-226

[9]T.A. Stolarski, Wei Chai (2006). Load-carrying capacity generation in squeeze film action. International Journal of Mechanical Sciences. 48(7), pp 736–741

[10]T.A Stolarski (2010). Numerical modelling and experimental verification of compressible squeeze film pressure. Tribology international. 43(1), pp 356-360

[11]Pinkuan Liu, Jin Li, Han Ding (2009). Modeling and experimental study on Near-Field Acoustic Levitation by flexural mode, IEEE Trans. Ultrason. Ferroelectr. Freq.Control. 56(12), pp 2679-2685

[12]Jin Li, Pinkuan Liu, Han Ding, Wenwu Cao (2011). Modeling characterization and optimization design for PZT transducer used in Near Field Acoustic Levitation. Sensors and Actuators A. 171(2), pp 260–265

[13]WEI Bin, MA Xizhi (2010). Research on the Characteristic of the Floating Guide Way with Squeeze Film. LUBRICATION ENGINEERING, 35(8), pp 54-58

[14]WEI Bin, MA Xizhi(2010).Research on the Characteristics of Squeeze Film Floating Guide Way Including the Model Effect. LUBRICATION ENGINEERING, 35(2), pp 33-35

[15]Jin Li, Wenwu Cao, Pinkuan Liu, and Han Ding(2010). Influence of gas inertia and edge effect on squeeze film in near field acoustic levitation. Appl. Phys. Lett. 96(24), 243507 pp 1-8

[16]W. J Xie, B. Wei (2012). Parametric study of single-axis acoustic levitation. Appl. Phys. Lett. 79(4), pp 881-886

[17]Mohamed Nabhani, Mohamed El Khlifi & Benyebka. Combined Non-Newtonian and Viscous Shear Effects on Porous Squeeze Film Behavior. Trabology Transactions. 55(4), pp 491-502

[18]T. V. V. L. N. Rao, A. M. A. Rani and T. Nagarajan etc(2013). Analysis of Journal Bearing with Double-Layer Porous Lubricant Film: Influence of Surface Porous Layer Configuration. Tribology Transactions. 56(5), pp 841-847

[19]A. Bouzidane & M. Thomas (2013). Nonlinear Dynamic Analysis of a Rigid Rotor Supported by a Three-Pad Hydrostatic Squeeze Film Dampers. Tribology Transactions. 56(5), pp 717-727

[20]YZ WANG, Bin WEI (2013). Mixed-modal Disk Gas Squeeze Film Theoretical and Experimental Analysis. International Journal of Modern Physics. 27(25), 1350168,pp 1-20

[21]R.C. Diprima, Asymptotic (1968). Methods for an Infinitely Long Slider Squeeze-film Bearing. J. Tribol. 90(1), pp 173-183

[22]H.Takada H.Miura (1983). Characteristics of Squeeze Air film Between Nonparallel Plates. ASME,J of Lubr.Technol 105(1), pp 147-151.

[23]Shigeaki.Kuroda,Noriyuki.Hirata (1984). The Characteristic of Motion of a round plate Supported on Squeeze Air Film.JSME, J of Lubr.,50(459), pp 2727-2731

[24]W.M.Beltman,P.J.M.Vander Hoogt(1997), J. Sound and Vibration, 206(2), pp 217-241

[25]A.Minikes, I.Bucher (2003). Coupled dynamics of a squeeze-film levitated mass and a vibrating piezoelectric disc: numerical analysis and experimental study. Journal of Sound and Vibration. 263(2), pp 241-268

[26]Ha, DN; Stolarski, TA; Yoshimoto,S (2005). An aerodynamic bearing with adjustable geometry and self-lifting capacity. Part 1: self-lift capacity by squeeze film. PROCEEDINGS OF THE INSTITUTION OF MECHANICAL ENGINEERS PART J-JOURNAL OF ENGINEERING TRIBOLOGY, 219(J1), pp 33-39

[27]Shigeka Yoshimoto,Hiroyuki Kobayashi,Masaaki Miyatake (2007), A non-contact chuck using ultrasonic vibration: analysis of the primary cause of the holding force acting on a floating object. Tribology International. 40(3), pp 503-511

[28]WEI Bin, MA Xizhi, TANG Weikun (2011), Study on Characteristics of Ultrasonic Levitation with Piezo-ceramics Exciting. PIEZOELECTRICS ACOUSTOOPTICS. 33(1), pp 71-78

[29]Stolarski, TA., Xue, Y. and Yoshimoto, S (2011)., Air journal bearing utilizing near-field acoustic levitation stationary shaft case. PROCEEDINGS OF THE INSTITUTION OF MECHANICAL ENGINEERS PART J-JOURNAL OF ENGINEERING TRIBOLOG . 225(3),:pp 120- 127

[30]YZ WANG, Bin WEI (2013). A Linear Solution for Gas Squeeze Film Characteristics in Ultrasonic Excitation Condition The journal of the Chinese society of mechanical engineers. 2013,34(5), pp 469-473

Nomenclature

y (m)	The width of plate actuator		L(m)	Width Variable
Y	The dimensionless form of y		p(pa)	Squeeze film pressure
t(s)	Time		p_0(Pa)	Atmospheric Pressure
T	The dimensionless form of t $$T=\omega t$$		P	The dimensionless form of p $$P=p/p_0$$
m(kg)	The mass of free levitation object		h_0(m)	Initial film thickness
f	Squeeze frequency		ω(rad/s)	Squeezing angular frequency $\omega=2\pi f$
μ(pa·s)	Dynamic viscosity		g(N)	Bearing force
σ	Squeeze Number $$\sigma = \frac{12\mu\omega b^2}{h_0^2 p_a}$$		F	Dimensionless bearing force $$F(T) = \frac{g(T)}{p_0 R_0^2}$$
h(m)	Film Thickness		X	The dimensionless form of x $$X=x/L$$
H	The dimensionless form of h $$H=h/h_0$$			

Appendix

1 The dimensionless film thickness equation derivation for plate actuator

The equation of wave shape in the coordinate in Fig.4 is

$y=a·sin[(2π*N/L)·x]$

Where, a is the amplitude of the plate shape, N is the wave number, L is the length of the plate, x is the position of the vibrating point.

Then, the film thickness equation is derived as

$h=h_0-y(x)= h_0- a·sin[(2π*N/L)·x]$

Where, h_0 is the initial film thickness, h is the simultaneous film thickness.

Use $Y=y/h_0$, $X=x/L$ $H=h/h_0$ to derive the dimensionless equations as follows

$H=1- Y(X)=1-a·sin(2πN·X)/h_0$

2 Governing equations of different squeeze film models for disc actuator

1) Fixed object (wall)

　　Dimensionless film thickness equation:

　　$H=1-\varepsilon\cos T$

　　Dimensionless Reynolds equation $\dfrac{H^3}{R}\dfrac{\partial}{\partial R}(RP\dfrac{\partial P}{\partial R}) = \sigma\dfrac{\partial(PH)}{\partial T})$

　　Where, $\sigma = \dfrac{12\mu\omega R_0^2}{p_0 h_0^2}$; $P = \dfrac{p}{p_0}$; $R = \dfrac{r}{R_0}$; $T = \omega t$; $H = \dfrac{h}{h_0}$

2) Free object levitation

　　Dimension film thickness equation:

　$H=1-\varepsilon\cos T+Y$

　　　Where, $y = h_0 Y$, $T = \omega t$, $h = h_0 H$, $\varepsilon = \delta h / h_0$

　　Dimensionless motion equation:

　　$\dfrac{d^2 Y}{dT^2} = \alpha(2\int_0^1 PRdR - 1 - W)$

Where, $\alpha = \dfrac{\pi p_a R_0^2}{m\omega^2 h_0}$ $W = \dfrac{w}{\pi R_0^2 p_a}$ $Y = \dfrac{y}{h_0}$ $T = \omega t$ $P = \dfrac{p}{p_a}$ $R = \dfrac{r}{R_0}$

3) Ideal flexuous wave exciting

　　Dimension film thickness equation:

　$H=(1-\varepsilon\cos-kR)+Y$

Where, $y = h_0 Y$, $T = \omega t$, $h = h_0 H$, $\varepsilon = \delta h / h_0$, $\Lambda = \lambda / 2R_0$ (dimensionless wave length), $k = 2\pi / \Lambda$

Dimensionless motion equation

$$\frac{d^2 Y}{dT^2} = \alpha \left(2\int_0^1 PR dR - 1 - W \right)$$

Where, $\alpha = \dfrac{\pi p_a R_0^2}{m\omega^2 h_0}$, $W = \dfrac{w}{\pi R_0^2 p_a}$, $Y = \dfrac{y}{h_0}$, $T = \omega t$, $P = \dfrac{p}{p_a}$, $R = \dfrac{r}{R_0}$

Dimensionless Reynolds equation $\dfrac{1}{R} \dfrac{\partial}{\partial R} \left(H^3 RP \dfrac{\partial P}{\partial R} \right) = \sigma \dfrac{\partial (PH)}{\partial T}$